Generation, Isolation, ESR and ^{1}H ENDOR Spectra, and Magnetic Characterization of *N*-[(4-Nitrophenyl)thio]-2-*t*-butyl-1-pyrenylaminyl[1)]

Yozo Miura,* Hiroyuki Oka, Eiji Yamano, Yoshio Teki,†

Takeji Takui,†† and Koichi Itoh†

Department of Applied Chemistry, Faculty of Engineering, Osaka City University, Sumiyoshi-ku, Osaka 558

†Department of Material Science, Faculty of Science, Osaka City University, Sumiyoshi-ku, Osaka 558

††Department of Chemistry, Faculty of Science, Osaka City University, Sumiyoshi-ku, Osaka 558

(Received September 20, 1994)

The oxidation of *N*-[(4-nitrophenyl)thio]-2-*t*-butyl-1-aminopyrene yielded a quite persistent and oxygen-insensitive *N*-[(4-nitrophenyl)thio]-2-*t*-butyl-1-pyrenylaminy radical (**3**), which was isolated as reddish-black fine needles. The hyperfine coupling (hfc) constants for the aminyl were determined by ESR and ^{1}H ENDOR measurements, indicating that there is an extensive delocalization of the unpaired electron from the nitrogen onto the pyrene ring. A comparison of the hfc constants with structurally close *N*-[(4-nitrophenyl)thio]-7-*t*-butyl-1-pyrenylaminyl (**1**) and *N*-[(4-nitrophenyl)thio]-2,7-di-*t*-butyl-1-pyrenylaminyl (**2**) showed that although the spin-density distribution of **3** is similar to that of **2**, it is greatly different from that of **1**. Magnetic susceptibility measurements of **3** in solid radical crystals showed that the magnetic interaction between the radical spins is strongly antiferromagnetic, giving $J/k=-108$ and -192 K for **2** and **3**, respectively.

For the past few years, isolable stable free-radicals have attracted widely growing interests from the viewpoints of both pure and applied chemistry because of the expectation that stable free radical crystals might behave as organic ferromagnets.[2)] As part of a program directed toward purely organic molecule-based magnetism,[3)] we have reported on the generation, stabilities, and ESR and ^{1}H ENDOR spectra of *N*-(arylthio)-7-*t*-butyl-1-pyrenylaminyls (**1**), *N*-(arylthio)-2,7-di-*t*-butyl-1-pyrenylaminyl (**2**), and *N*-(arylthio)-1-pyrenylaminyl (**5**).[4)] Although aminyls **5** were less persistent than expected [half-lifetime, <1 h (benzene, 20 °C)], sterically protected **1** and **2** were much more persistent; particularly interesting was **2**, which was isolated as radical crystals. As an extension of this study we have investigated 2-*t*-butyl-1-pyrenylaminyl (**3**), because, in spite of the absence of a *t*-butyl group at C7 of the pyrene ring, aminyl **3** is quite persistent and can be isolated as radical crystals, similar to **2** (Chart 1). In this paper we report on the generation, isolation, ESR and ^{1}H ENDOR spectra, as well as the magnetic characterization of **3**.

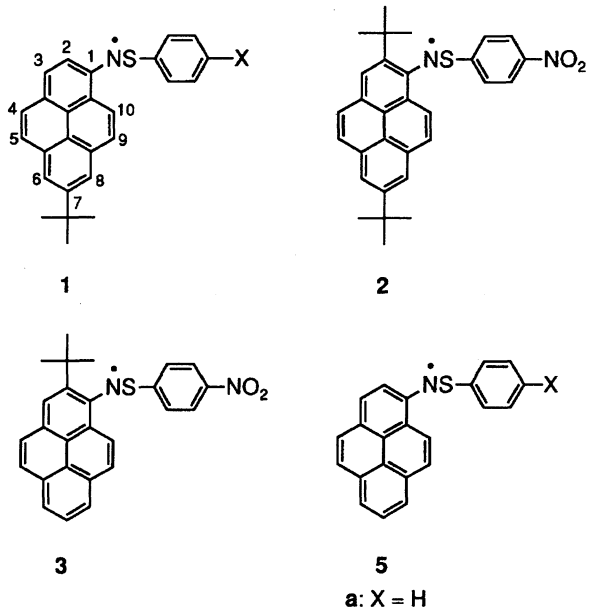

Chart 1.

Results and Discussion

Generation and ESR and ^{1}H ENDOR Spectra of 3. Precursor **4** was prepared according to the route shown in Scheme 1. Upon a treatment of 2-*t*-butylpyrene with concd HNO_3 in acetic acid, 2-*t*-butyl-1-nitropyrene and 7-*t*-butyl-1-nitropyrene were obtained in 33 and 56% yields, respectively. 2-*t*-Butyl-1-nitropyrene was then reduced with 5%-Pd/C under a hydrogen atmosphere to give 1-amino-2-*t*-butylpyrene in 45% yield. The aminopyrene was allowed to react with 4-nitrobenzenesulfenyl chloride in the presence of trieth-

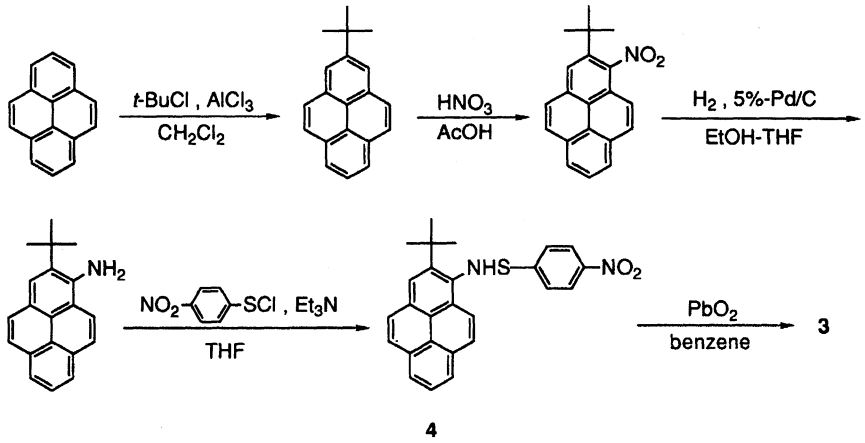

Scheme 1.

ylamine to give **4** in 26% yield.

The generation of **3** was accomplished by PbO_2 oxidation of **4**. When PbO_2 was added to a light-yellow solution of **4** in benzene, it immediately turned dark red and gave an intense ESR signal due to **3**. The ESR spectrum was very complex and broad due to the presence of many unequivalent protons as shown in Fig. 1. We therefore measured the ^{1}H ENDOR spectrum of **3** in toluene at −90 °C. A high-resolution ENDOR spectrum with a good S/N ratio was obtained by 200-times accumulation with a low-frequency modulation depth (50 kHz). As shown in Fig. 2, the ENDOR spectrum gave eight pairs of peaks. The innermost pair of peaks

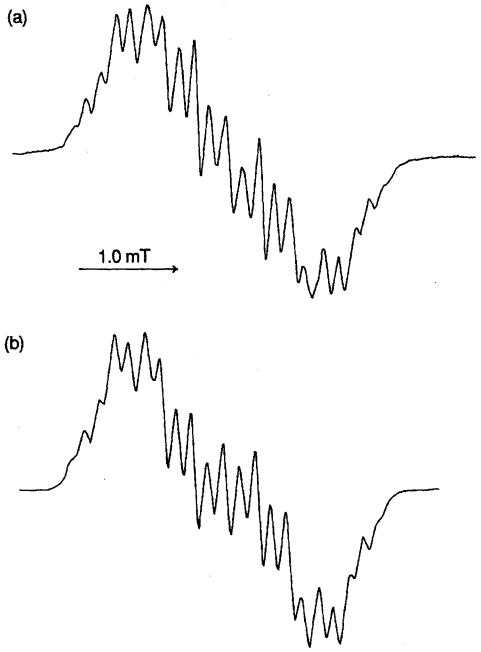

Fig. 1. Observed (upper) and computer simulated (bottom) ESR spectra of **3**. The observed spectrum was obtained using benzene as a solvent at 20 °C. The computer simulated spectrum was reconstructed using the hfc constants in Table 1 and the linewidth of 0.071 mT.

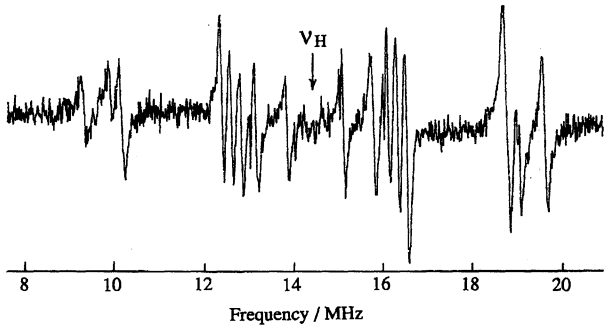

Fig. 2. ^{1}H ENDOR spectrum of **3** in toluene at −90 °C.

was assigned to the ortho protons of the benzene ring, and the remaining seven pairs of peaks to the protons of the pyrene ring. Since the pyrene ring has eight aromatic protons, two pairs of peaks completely overlap into a pair of single peaks. The overlapping peaks were found to arise from the protons with a hfc constant of 8.57 MHz (0.305 mT) by means of computer simulation of the observed ESR spectrum (Fig. 1). The hfc constants and g value determined for **3** are summarized in Table 1.

The actual assignment of the protons was difficult without a partial deuteration of the pyrene-ring protons. However, the following rough assignment of the protons was possible based on the spin-density distribution predicted by McLachlan–Hückel MO calculations performed for *N*-(phenylthio)-1-pyrenylaminyl (**5a**), assuming that it is planar.[5] As indicated in Table 1, the four pyrene ring protons having larger hfc constants were assigned as H_5, H_6, H_8, and H_9, while the remaining four protons having smaller hfc constants were assigned as H_3, H_4, H_7, and H_{10}.

Isolation of 3. Although aminyl **3** does not have a *t*-butyl group at C7, it was found to be surprisingly persistent. This was demonstrated by a simple kinetic ESR study. Its benzene solution was put into an ESR cell and the double-integrated ESR signals were measured at 20 °C as a function of time under atmospheric conditions. Although the ESR measurements were con-

Table 1. Hyperfine Coupling Constants and g Value for **3** and Comparison of Those with **1** and **2**

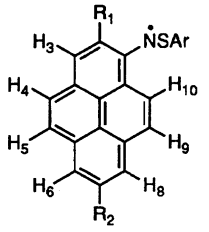

1a: $R_1=H_2$, $R_2=t$-Bu, Ar=4-$NO_2C_6D_4$
2: $R_1=R_2=t$-Bu, Ar=4-$NO_2C_6H_4$
3: $R_1=t$-Bu, $R_2=H_7$, Ar=4-$NO_2C_6H_4$
5a: $R_1=H_2$, $R_2=H_7$, Ar=Ph

Radical	a_N/mT[a]	a_H/mT		a_{other}/mT	g
		H_2, H_5, H_6, H_8, H_9[b]	H_3, H_4, H_7, H_{10}[c]		
1a[d,e]	0.848	0.270, 0.245, 0.238, 0.230, 0.220	0.147, 0.117, 0.117		2.0046
2[d,e]	0.664	0.363, 0.316, 0.302, 0.298	0.152, 0.150, 0.126	0.041[f,g]	2.0043
3[e]	0.662	0.363, 0.326, 0.304, 0.304	0.152, 0.137, 0.119, 0.093	0.046[f]	2.0043
3[h]		0.367, 0.326, 0.305, 0.305	0.149, 0.133, 0.117, 0.093	0.046[f]	
5a[i]	0.755	0.281 (H_2), 0.251 (H_5), 0.251 (H_6), 0.251 (H_8), 0.254 (H_9)	−0.089 (H_3), −0.073 (H_4), −0.054 (H_7), −0.073 (H_{10})	0.051[f]	

a) The value for the central nitrogen. b) For **1a** the values of H_2, H_5, H_6, H_8, and H_9 are given, and for **2** and **3** the values for H_5, H_6, H_8, and H_9 are given. c) For **1a** and **2** the values of H_3, H_4, and H_{10} are given, and for **3** the values of H_3, H_4, H_7, and H_{10} are given. d) Ref. 4. e) The hfc constants determined by ESR. f) The value for the ortho protons of the phenylthio group. g) When Ar is p-$NO_2C_6D_4$, the complete disappearance of this hyperfine coupling was observed (see: Ref. 4). h) The hfc constants determined by ENDOR. i) The hfc constants predicted by the McLachlan–Hückel MO calculations using the McConnell equation ($a_X=Q_X\rho_X$, where $Q_N=2.2$ and $Q_H=-2.7$ mT; see Ref. 5).

tinued for 10 h, no reduction in the signal intensity was observed, indicating that **3** is a quite persistent and oxygen-insensitive radical. Furthermore, **3** showed no tendency to dimerize, even upon cooling to −50 °C in solution. These interesting results prompted us to isolate **3**.

Isolation was performed by the following procedure. Precursor **4** was oxidized with PbO_2 in benzene. After filtration, the solvent was removed by freeze-drying, and the resulting dark-red powder was recrystallized from benzene–hexane to give reddish-black fine needles in 28% yield.

The structure of **3** was confirmed based on its satisfactory elemental analysis and its IR spectrum. Although the IR spectrum of **4** showed a strong absorption due to the stretching vibration of N–H was observed at 3350 cm^{-1}, no NH absorption was observed in that of **3**. The purity of this radical was determined to be 95% by the solution ESR measurements using 1,3,5-triphenylverdazyl as a reference.

Comparison of ESR Parameters of 3 with Those of 1 and 2. In Table 1 the hfc constants and the g value for **3** are compared with those of **1** and **2**. The hfc constants and the g value for **3** are very close to those of **2**, but quite different from those of **1**. This indicates that the spin-density distribution of **3** is very similar to that of **2**, but largely different from that of **1**. In a previous paper[4] we reported that the unpaired electron is more extensively delocalized from the central nitrogen to the pyrene ring in **2** than in **1**. This conclusion was based on the ESR results in which a smaller a_N value and larger a_H values of the pyrene ring protons were observed for **2** than for **1**. It is thus concluded that **3** as well as **2** adopt a more planar conformation than that of **1**. We thus assume that, in **1**, the pyrene ring is more twisted about the C1–N bond. We presently have no reasonable explanation concerning the reason why **2** and **3** take a more planar conformation than **1**, in spite of the larger steric effect of the t-butyl group around the radical center. An X-ray crystallographic analysis of **2** or **3**, compared with that of **1**, may solve this question.[6]

UV-visible Spectrum. Aminyl **3** is characterized by its red color. As found in Fig. 3, **3** absorbs at 498 (ε 25600), 474 (sh, 22800), and 414 nm (15900) in the visible region and at 392 (sh, 9830), 359 (10700), and 314 nm (11100) in the UV region. The strong absorption at 498 nm is ascribable to the characteristic red

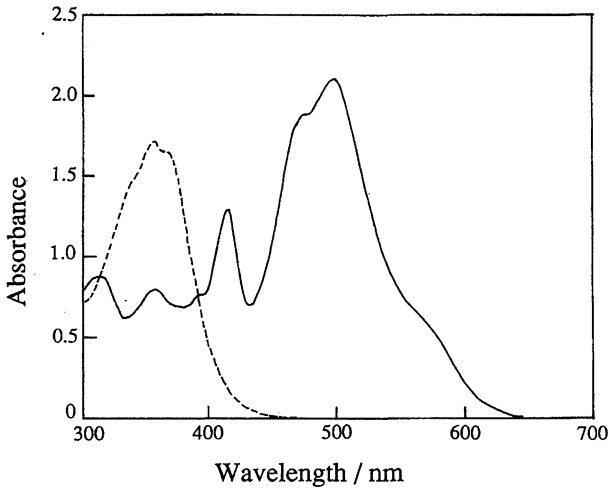

Fig. 3. UV-visible spectra of **3** and **4** in benzene. (—): **3** (8.63×10^{-5} mol dm^{-3}); (---): **4** (7.17×10^{-5} mol dm^{-3}).

color of **3**. It was confirmed that precursor **4** has no absorption in the visible region. Accordingly, the radical concentration of **3** can be determined by measuring the absorption at 498 nm.

Role of the 2-*t*-Butyl Group as a Protector for the Stabilization of 3. Before starting this study, we had supposed that the *t*-butyl group at C7 plays an important role in the steric protection, because there are two positions (C6 and C8) with high spin densities next to C7. Unexpectively, however, aminyl **3** is exceptionally stable and can be isolated as radical crystals in spite of the absence of the *t*-butyl group at C7. There is therefore no doubt that the *t*-butyl group at C7 does not play an important role as a protector. On the other hand, the importance of the *t*-butyl group at C2 as a protector can be seen from the large difference in the stability between **1** and **2**. It is therefore obvious that the substitution at C2 plays important roles in the unusual stabilization of **2** and **3**. Its primary role may be a steric protection of the radical center from reversible and irreversible homolytic reactions, including dimerization at N producing a N–N coupled dimer. Another important role may be to make **2** and **3** to adopt a more planar conformation, leading to a greater electronic stability, although the mechanism has not yet been clarified.

Magnetic Susceptibility Measurements of Radical Crystals. The magnetic behavior of stable *N*-thioaminyl radical crystals has for the first time been investigated for *N*-(arylthio)-(2,4,6-triphenylphenyl)-aminyl radicals on a SQUID magnetometer in the 1.8—300 K temperature range,[7] and strong antiferromagnetic intermolecular interactions among the radicals in the crystals were observed. For example, the magnetic behavior of *N*-[(3-nitrophenyl)thio]-(2,4,6-triphenylphenyl)aminyl radical crystals was well interpreted in terms of the following alternating-linear-chain model of an antiferromagnetic interaction[8] with $J/k=-26$ K and $\alpha=0.92$:

$$\mathcal{H}=-2J\sum(S_{2i}S_{2i-1}+\alpha S_{2i}S_{2i+1}). \quad (1)$$

In this case, the extensive delocalization of an unpaired π-electron spin and the overlapping between the π-SOMOs (singly occupied molecular orbital) of the neighboring radicals may be responsible for such a strong antiferromagnetic intermolecular interaction.

In the present pyrene-ring bearing thioaminyl radicals **2** and **3** there is a more extensive delocalization of the unpaired π-electron spin from the nitrogen to the pyrene group. Hence, a larger overlapping between the π-SOMOs of the neighboring radicals is expected. Molar magnetic susceptibility (χ_{mol}) measurements of **2** and **3** were carried out on a SQUID magnetometer in the 1.8—300 K temperature range. The purities of **2** and **3** used in the magnetic susceptibility measurements were determined by ESR to be 94 and 95%, respectively. χ_{mol} vs. T plots of **2** are shown in Fig. 4. When the temperature was lowered from 300 K, χ_{mol} increased slightly, and then slightly decreased; below 50 K it significantly increased. This significant increase is probably due to isolated monoradicals which are randomly located in the lattice. The χ_{mol} vs. T plots were analyzed in terms of both the alternating infinite linear-chain model (Eq. 1) and the singlet-triplet model. In both models the amounts of isolated monoradicals in the lattice are taken into account. A best fit with the experimental plots was obtained when a theoretical curve was drawn by the alternating infinite linear-chain model with $J/k=-108.2$ K and $\alpha=0.827$, assuming the amounts of isolated monoradicals in the lattice to be 5.4%, though there still remain large deviations between the experimental plots and the theoretical curve. In this system spin pairing takes place to a great extent due to the large antiferromagnetic interaction, even at high temperature. This means that the errors in the estimation of the diamagnetic components and of the amounts of paramagnetic impurities significantly affect the magnitudes of the absolute values of χ_{mol}. The deviations between the experimental plots and the theoretical curve in Fig. 4 may therefore arise due to the difficulty to extract the net paramagnetic susceptibility of **2**. Similar χ_{mol} vs. T plots were also obtained for **3**; the experimental plots were best fitted by using the alternating infinite linear-chain model with $J/k=-191.8$ K and $\alpha=0.874$, assuming the amounts of monoradicals isolated in the lattice to be 2.8%, though large deviations between the experimental plots and the theoretical curve were still observed, similar to the case of **2**. The greater antiferromagnetic coupling of **3** can be interpreted in terms of the absence of the 7-*t*-butyl group, because a greater overlapping between the π-SOMOs of the neighboring radicals is possible.[9] Because of the unusually strong antiferromagnetic intermolecular interactions of **2** and **3**, the $\chi_{mol}T$ vs. T curves

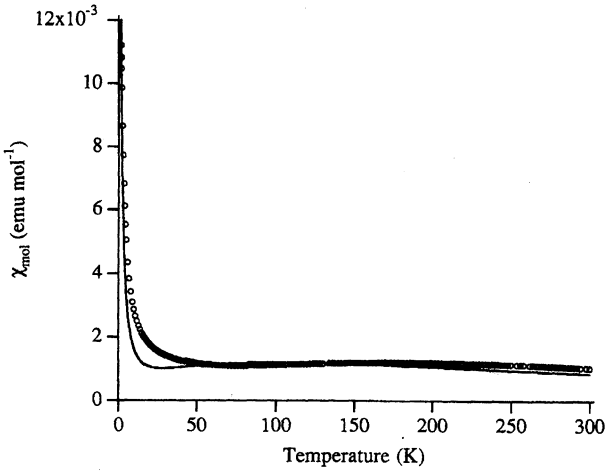

Fig. 4. χ_{mol} vs. T plots of **2** in solid radical crystals. The solid curve is the theoretical fit (see, text).

still increased with temperature, even at 300 K, in both cases. The $\chi_{mol}T$ values at 300 K are 0.32 (**2**) and 0.21 emu K mol^{-1} (**3**), respectively, which are considerably lower than the theoretical value for paramagnetic monoradicals (0.376 emu K mol^{-1}).

Experimental

The melting points were determined on a Yanagimoto micro melting-point apparatus and are uncorrected. IR spectra were obtained on a JASCO A-202 spectrophotometer. UV-visible spectra were recorded on a Shimadzu (UV-2200) spectrophotometer. ^{1}H NMR spectra were measured with a JEOL (α-400) spectrometer (400 MHz); chemical shifts are expressed in ppm values (δ) using Me_4Si as an internal standard. ESR spectra were measured on a JEOL (JES-ME-3X) or Bruker (ESP 300) spectrometer equipped with an X-band microwave unit and with a 100 kHz field modulation. The hyperfine coupling constants and g values were determined by a simultaneous measurement of Fremy's salt in a dilute K_2CO_3 aqueous solution (a_N=1.309 mT; g=2.0057) as a reference.

The spin concentrations of **2** and **3** were determined by double integration of the ESR spectra of the sample and reference in benzene solutions. The calibration curve was drawn with a solution of 1,3,5-triphenylverdazyl using the same ESR cell, the same solvent, and the same instrument settings as for the sample measurements.

^{1}H ENDOR measurements were carried out at −90 °C on a Bruker (300/350) ENDOR spectrometer equipped with a TM_{011} mode microwave cavity operating at X-band using toluene as a solvent.

Magnetic susceptibility measurements were carried out with a Quantum Design SQUID magnetometer (MPMS2) in the 1.8—300 K temperature range. The diamagnetic contributions of the samples were estimated from the Pascal's diamagnetic constants.

2-*t*-Butylpyrene was obtained by our previously reported method.[4] 4-Nitrobenzenesulfenyl chloride was prepared from 4,4′-dinitrodiphenyl disulfide by treating with chlorine in dichloromethane.

2-*t*-Butyl-1-nitropyrene: This nitro compound was obtained according to a procedure reported by Cornelisse et al., with some modifications.[10] A suspension of 12.7 g (49 mmol) of 2-*t*-butylpyrene in 200 cm^3 of acetic acid was heated to 100—110 °C with stirring to become homogeneous. After 3.74 cm^3 of concd HNO_3 was added in one portion, the resulting dark-red solution was heated at the same temperature for 1 h, cooled, and poured into a large excess of ice-water. The orange powder product was collected by filtration, washed with water, and dissolved in 200 cm^3 of dichloromethane. The dichloromethane solution was washed with 1 M NaOH (1 M=1 mol dm^{-3}) and water, and dried ($MgSO_4$). After evaporation, the residue was chromatographed on a silica gel-column (Wako gel, C200) with 1:2 benzene–hexane as an eluant. The more mobile light-yellow zone gave 2-*t*-butyl-1-nitropyrene and the less mobile zone gave 7-*t*-butyl-1-nitropyrene. Crystallization from hexane–benzene gave 2-*t*-butyl-1-nitropyrene as yellow needles in 33% yield (4.91 g, 16.2 mmol). Mp 181—183 °C; ^{1}H NMR ($CDCl_3$) δ=1.64 (s, *t*-Bu, 9 H), 7.75 (d, J=9.2 Hz, aromatic, 1 H), 8.03 (d, J=9.2 Hz, aromatic, 1 H), 8.04 (t, J=7.3 Hz, aromatic, 1 H), 8.12 (d, J=9.2 Hz, aromatic, 1 H), 8.16 (d, J=9.2 Hz, aromatic, 1 H), 8.22 (d, J=7.3 Hz, aromatic, 1 H), 8.23 (d, J=7.3 Hz, aromatic, 1 H), and 8.30 (s, aromatic, 1 H).

1-Amino-2-*t*-butylpyrene: 2-*t*-Butyl-1-nitropyrene (5.0 g, 16.5 mmol) was dissolved in THF (200 cm^3)–ethanol (200 cm^3) with stirring. After 5%-Pd/C (6.0 g) was added, hydrogen was bubbled into the solution for 2—3 h at room temperature with stirring. After filtration, the filtrate was evaporated under reduced pressure and the residue was chromatographed on a silica-gel column (Wako gel, C200) with 1:1 benzene–hexane. Crystallization from hexane–benzene gave golden plates in 45% yield (2.05 g, 7.5 mmol). Mp 137—139 °C; IR (KBr) 3470 and 3390 cm^{-1} (NH_2); ^{1}H NMR ($CDCl_3$) δ=1.65 (s, *t*-Bu, 9 H), ca. 4.2 (br, NH_2, 2 H), and 7.88—8.09 (m, aromatic, 8 H).

***N*-[(4-Nitrophenyl)thio]-2-*t*-butyl-1-aminopyrene (4):** To a stirred solution of 1.00 g (3.7 mmol) of 1-amino-2-*t*-butylpyrene and 2.0 cm^3 of triethylamine in 100 cm^3 of anhydrous THF was added dropwise a solution of 1.38 g (7.3 mmol) of 4-nitrobenzenesulfenyl chloride in 10 cm^3 of anhydrous THF at 0 °C. After being stirred for 2 h at 0 °C, the reaction mixture was filtered, and the filtrate was evaporated under reduced pressure. The residue was chromatographed on alumina column (Merck, aluminium oxide 90) with 1:2 hexane–benzene. Crystallization from benzene gave yellow prisms in 26% yield (0.41 g, 0.96 mmol). Mp 178—180 °C; IR (KBr) 3350 cm^{-1} (NH); UV (benzene) λ_{max}=366 (ε=23200) and 356 nm (24100); ^{1}H NMR ($CDCl_3$) δ=1.76 (s, *t*-Bu, 9 H), 5.96 (s, NH, 1 H), 7.77 (d, J=9.1 Hz, phenyl, 2 H), 7.84 (d, J=9.2 Hz, pyrenyl, 1 H), 7.93 (t, J=7.3 Hz, pyrenyl, 1 H), 7.98 (s, pyrenyl, 2 H), 8.05 (d, J=9.2 Hz, pyrenyl, 1 H), 8.06 (d, J=7.3 Hz, pyrenyl, 1 H), 8.11 (d, J=7.3 Hz, pyrenyl, 1 H), 8.18 (s, pyrenyl, 1 H), and 8.34 (d, J=9.1 Hz, phenyl, 2 H). Found; C, 73.18; H, 5.30; N, 6.38%. Calcd for $C_{26}H_{22}N_2O_2S$: C, 73.21; H, 5.20; N, 6.57%.

***N*-[(4-Nitrophenyl)thio]-2-*t*-butyl-1-pyrenylaminyl (3):** After compound **4** (100 mg, 0.234 mmol) was dissolved in 12 cm^3 of benzene with stirring, 1.0 g of K_2CO_3 was added. Then, PbO_2 (1.0 g) was added in some portions for 2 min; the resulting dark-red mixture was further stirred for 0.5 min. After filtration, the solvent was removed by freeze-drying, and benzene (ca. 1 cm^3) was added. The resulting dark-red solution containing undissolved radical crystals was heated to the reflux temperature, and hexane (ca. 20 cm^3) was added. Upon cooling to 0 °C reddish-black fine needles were given in 28% yield (28 mg, 0.066 mmol). Mp 192—193 °C; IR (KBr) 2950, 2900, 1590, 1570, 1510, 1470, 1335, 1255, 1235, 1170, 1110, 1080, 890, 855, 840, 820, 740, 680, and 600 cm^{-1}; UV-vis (benzene) λ=498 (ε=25600), 474 (sh, 22800), 414 (15900), 392 (sh, 9830), 359 (10700), and 314 nm (11100). Found: C, 73.15; H, 5.12; N, 6.72%. Calcd for $C_{26}H_{21}N_2O_2S$: C, 73.39; H, 4.97; N, 6.58%.

This work was supported (in part) by a Grant-in-Aid for Scientific Research on Priority Area "Molecular Magnetism" (Area Nos. 228/05226231 and 06218226) from the Ministry of Education, Science and Culture.

References

1) ESR Studies of Nitrogen-Centered Free Radicals. 47. Part 46: Y. Miura and E. Yamano, *J. Org. Chem.*, **60**, 1070 (1995).

2) M. Kinoshita, P. Turek, M. Tamura, K. Nozawa, D. Shiomi, Y. Nakazawa, M. Ishikawa, M. Takahashi, K. Awaga, T. Inabe, and Y. Maruyama, *Chem. Lett.*, **1991**, 1225; R. Chiarelli, M. A. Novak, A. Rassat, and J. L. Tholence, *Nature*, **363**, 147 (1993); T. Nogami, K. Tomioka, T. Ishida, H. Yoshikawa, M. Yasui, F. Iwasaki, H. Iwamura, N. Takeda, and M. Ishikawa, *Chem. Lett.*, **1994**, 29; T. Ishida, H. Tsuboi, T. Nogami, H. Yoshikawa, M. Yasui, F. Iwasaki, H. Iwamura, N. Takeda, M. Ishikawa, *Chem. Lett.*, **1994**, 919; T. Sugawara, M. M. Matsushita, A. Izuoka, N. Wada, N. Takeda, and M. Ishikawa, *J. Chem. Soc., Chem. Commun.*, **1994**, 1723.

3) For recent papers; see: Y. Miura, M. Matsumoto, and Y. Ushitani, *Macromolecules*, **26**, 2628 (1993); Y. Miura, Y. Ushitani, K. Inui, Y. Teki, T. Takui, and K. Itoh, *Macromolecules*, **26**, 3698 (1993); Y. Miura, M. Matsumoto, Y. Ushitani, Y. Teki, T. Takui, and K. Itoh, *Macromolecules*, **26**, 6673 (1993); Y. Miura and Y. Ushitani, *Macromolecules*, **26**, 7079 (1993); Y. Miura, Y. Ushitani, M. Matsumoto, K. Inui, Y. Teki, T. Takui, and K. Itoh, *Mol. Cryst. Liq. Cryst.*, **232**, 135 (1993).

4) Y. Miura, E. Yamano, A. Tanaka, and J. Yamauchi, *J. Org. Chem.*, **59**, 3294 (1994).

5) The following parameters were used for the MO calculations: $\alpha_N=\alpha+0.6\beta$, $\alpha_S=\alpha+\beta$, $\beta_{CN}=1.1\beta$, $\beta_{NS}=0.7\beta$, $\beta_{CS}=0.7\beta$, $\lambda=0.7$: Y. Miura, H. Asada, M. Kinoshita, and K. Ohta, *J. Phys. Chem.*, **87**, 3450 (1983).

6) We have not yet obtained a single crystal of **2** or **3** large enough for X-ray crystallographic analysis.

7) Y. Teki, Y. Miura, A. Tanaka, T. Takui, and K. Itoh, *Mol. Cryst. Liq. Cryst.*, **233**, 119 (1993).

8) W. Duffy, Jr., and K. P. Barr, *Phys. Rev.*, **165**, 647 (1968).

9) Recently, similarly large antiferromagnetic couplings for organic free radicals were observed. For example : T. Barth, B. Banellakopulos, C. Krieger, and F. A. Neugebauer, *J. Chem. Soc., Chem. Commun.*, **1993**, 1626; K. Mukai, K. Inoue, N. Achiwa, J. B. Jamali, C. Krieger, and F. A. Neugebauer, *Chem. Phys. Lett.*, **224**, 569 (1994).

10) L. Rodenburg, R. Brandsma, C. Tintel, J. van. Thuijl, J. Lugtenburg, and J. Cornelisse, *Recl. Trav. Chim. Pays-Bas*, **105**, 156 (1986).